



Cardiac CT and Structural Heart Disease Interventions (Non-TAVI)

Christina Tan¹ · Dee Dee Wang² · Mark Reisman¹ · Jacqueline Saw³

Published online: 19 October 2019

© Springer Science+Business Media, LLC, part of Springer Nature 2019

Abstract

Purpose of review The use of cardiac CT is well established in the TAVR sphere and gaining traction as an integral part of pre-procedural planning for left atrial appendage closure (LAAC) and transcatheter mitral valve replacement (TMVR). We aim to review the recent evidence regarding the accuracy of cardiac CT for left atrial sizing and device selection and discuss the contribution of cardiac CT to decreasing complication rates in real-world experience as compared with clinical trials.

Recent findings Pre-procedural CT imaging has evolved to become an integral part of LAA closure and TMVR. For LAA closure, CT imaging provides detailed anatomic assessment of the LAA and surrounding structures and accurate measurements for device sizing. These can facilitate device and equipment selection and enhance safety and outcomes with intraprocedural guidance with transesophageal echocardiography or intracardiac echocardiography. For TMVR, pre-procedural CT is necessary to assess the potential risk of LVOT obstruction and determine device sizing. Such assessments can help pre-plan the potential need for adjunctive strategies to lower the risk of LVOT obstruction.

Summary CT imaging has gained important roles in the field of structural interventions, and understanding how to utilize this tool is an important skill to acquire as a contemporary comprehensive interventionist. Pre-procedural CT imaging has evolved to become an integral part of LAA closure and TMVR.

Keywords Left atrial appendage closure · Structural heart disease interventions · Cardiac computed tomography · Transcatheter mitral valve replacement · Atrial fibrillation

CT Angiography for Left Atrial Appendage Closure

Introduction

Atrial fibrillation (AF) is a growing global health burden, affecting 1.5 to 2% of the general population and increasing in prevalence [1]. It is a major cause of stroke, with > 90% of

non-valvular AF-related left atrial thrombi isolated to the left atrial appendage (LAA) [2]. Thus, efforts for developing and implanting devices to isolate the LAA have been in fervent development over the past 20 years. Of these, the WATCHMAN device (Boston Scientific, Marlborough, Massachusetts) was approved by the FDA in 2015 for LAA closure to reduce the risk of stroke in patients with non-valvular AF, following data from the randomized-controlled studies, PROTECT-AF (Watchman Left Atrial Appendage System for Embolic Protection in Patients with Atrial Fibrillation) and PREVAIL (Prospective Randomized Evaluation of the Watchman LAA Closure Device in Patients with Atrial Fibrillation Versus Long-Term Warfarin Therapy) [3].

Wang and DiBiase et al. [4] first described the commonly recognized LAA morphologies in use today (Table 1). The LAA is a highly variable structure and can have multiple lobes, angulations, and extensive trabeculations. Understanding the anatomy can facilitate selecting and implanting LAA closure devices, which can help improve the safety and efficiency of performing these procedures. The original clinical trials [3, 5]

This article is part of the Topical Collection on *Cardiac Computed Tomography*

✉ Jacqueline Saw
jsaw@mail.ubc.ca

¹ Division of Cardiology, University of Washington, Seattle, Washington, USA

² Division of Cardiology, Henry Ford Hospital, Detroit, MI, USA

³ Division of Cardiology, Vancouver General Hospital, University of British Columbia, Columbia, 2775 Laurel Street, Level 9, Vancouver, BC V5Z 1M9, Canada

Table 1 LAA morphologies

LAA morphology	Characterization
Chicken wing	Obvious bend present in the proximal or middle dominant lobe
Windsock	Dominant lobe without any obvious bend or branches
Cauliflower	Limited overall LAA length with a number of significant lobes and potentially lack of 1 dominant lobe
Cactus	Dominant central lobe with secondary lobes in superior and inferior directions

were performed with transesophageal echocardiography (TEE) for pre-procedural planning as well as intraprocedural guidance. While 2-dimensional (2D) TEE is the most commonly used imaging modality, the use of 3-dimensional (3D) imaging has distinct advantages compared with 2D-TEE alone. CT angiography (CTA) is non-invasive and provides superior 3D depiction of the LAA and surrounding structures and accurate sizing of the LAA for device selection. Thus, CTA is increasingly used for baseline imaging for LAA closure pre-planning.

CTA Protocol

The type of CTA protocol utilized plays an important role in improving LAA sizing accuracy. Since the left atrium is a highly compliant chamber, the volume status of the patient will impact LAA sizing. Thus, adequate hydration with oral intake or saline infusion should be administered before scanning to maximize chamber dimensions. There is also variation in dimensions throughout the cardiac cycle, and imaging and

measurements should be taken at the cardiac phase with the largest LAA dimension, which is usually at late atrial diastole (late ventricular systole) corresponding to 30–40% of the RR interval [6].

Different CT machines and protocols were reported for LAA assessment in the literature. At least 64-detector scanners should be used, and settings can include rotation time 400 ms, collimation 64×0.5 mm, tube voltage 100–135 kV, and tube current 250–400 mA. It is preferable to utilize 320-detectors for more detailed LAA assessment, and the settings can include rotation time 350 ms, collimation 320×0.5 mm, tube voltage 100–135 kV, and tube current 400–580 mA. Another advantage of 320 detectors is avoidance of step artifacts with irregular AF rhythm. Either prospective ECG-triggered dose modulation or retrospective-gating can be used. Examples of CTA protocols are listed in Table 2. Beta-blockade is usually not required for LAA assessment. The volume of non-ionic contrast should be dependent on body weight, total scan time, and renal function, but typically range from 50 to 90 cm³.

Table 2 Sample CCTA protocol for LAA pre-procedure and post-surveillance imaging

	Prospective cardiac-gated protocol	Retrospective cardiac-gated protocol
Tube potential	100 kV for BMI < 30 120 kV if BMI > 30	
Tube current	300–500 mA	
Scan direction	Cranial to caudal	
Scan volume	Heart to diaphragm (14–16 cm)	
Size	512 mm	
Detector collimation	320×0.5	
Cardiac phase-reconstruction	30–40% RR interval or 250 ms after R wave	5–95% valve cine series, mid to late ventricular systole
Bolus tracking	Sure start	
Contrast injection	50–80 cm ³ contrast + 50 cm ³ 30% contrast and saline mixture (5 cm ³ /s)	80 cm ³ contrast (4 cm ³ /s)
Saline injection	IV saline injection (5 cm ³ /s) 30 cm ³ saline	
Heart rate	No restriction	
B-blocker and nitrates	Not required	

Adapted from Saw et al. CCTA for Left Atrial Appendage Closure. CJC (2016) 8 [7] and Wang et al. 3DRCT for Watchman. JACC Cardiovascular Intervention 2016; 9, 22 [8]

BMI body mass index, CCTA cardiac computed tomography angiography, IV intravenous, LAA left atrial appendage

Digital Post-processing

Several image processing commercial software are available for manual and automated reconstruction of the CTA images of the LAA and surrounding structures. These include VitreaWorkstation™ (Vital, Toshiba Medical Systems Group Company, the Netherlands), Aquarius Workstation (TeraRecon Inc., Foster City, CA), Brilliance Workspace (Philips Healthcare, Andover, MA), and 3mensio software (3mensio Medical Imaging, the Netherlands).

To assess for suitability and sizing for LAA closure, baseline assessment of the shape and dimensions of the LAA is important. Multiplanar reformat (MPR) oblique planes are typically used for measurements. To measure the LAA ostium, an oblique MPR plane is selected where the circumflex artery, the pulmonary vein ridge, and the LAA ostium can be clearly seen. For the WATCHMAN device, the ostium of the LAA is measured from the circumflex artery to a superior point 1–2 cm within the pulmonary vein ridge. The crosshair is positioned at the ostium, in co-axial fashion with the wall of the appendage. The crosshair is then adjusted at an orthogonal plane, again to be co-axial with the LAA wall. The remaining orthogonal double-oblique plane then projects the enface view of the LAA, where the minimum and maximum diameters of the LAA orifice can be measured (Fig. 1). The depth of the LAA can also be obtained on MPR or with maximal intensity projection (MIP), choosing an oblique plane where the ostium and the distal tip of the LAA can be visualized. 3D volume-rendered images can also be produced, which provides more

detailed assessment of the LAA shape and branches, and can also aid selection of fluoroscopic angles to guide device implantation (Fig. 2).

Comparing CTA to TEE Measurements

3D imaging with CTA or 3D-TEE provides more accurate measurements of the LAA ostium and depth, given that the LAA orifice and body can be highly variable in shape [8]. An observational study of 28 patients by Zhou et al. [9] demonstrated that measurement by 3D-TEE yielded larger landing zone dimensions compared with 2D-TEE (22.6 ± 5.7 mm vs. 20.9 ± 5.1 mm, $p < 0.001$). 3D-TEE correlated better with CTA but was still undersized ($p = 0.022$). Depth dimensions by 2D-TEE were similarly smaller than 3D-TEE (27.7 ± 4.5 mm vs. 28.9 ± 4.5 mm, $p = 0.009$) and CT (27.7 ± 4.5 mm vs. 32.0 ± 4.3 mm, $p < 0.001$), while the difference in CTA sizing vs 3D-TEE sizing continued to be statistically significant ($p < 0.001$). Similar findings were reported by Saw et al. [10], where maximal LAA diameter was significantly larger for CTA (24.1 ± 4.7 mm) versus TEE (22.3 ± 4.9 mm) ($p < 0.001$), and by Chow et al. [11], where CTA findings predicted the correct device in 83% of cases, compared with 57% for 2D-TEE. Rajwani et al. [12] also found CTA sizing to be more predictive of final device size compared with 2D-TEE.

Reliability of CTA imaging compared with 3D-TEE was supported in a small study of 30 patients [13] who found no significant difference in area of LAA orifice (3.0 ± 0.8 cm² and 3.2 ± 1.1 cm², $p = 0.4$) or maximal LAA diameter (24.0

Fig. 1 Multiplanar reformat images of a retroflex chicken wing anatomy: **a** oblique coronal plane with crosshair aligned with the wall of the LAA at the orifice; **b** 2nd oblique plane with crosshair adjusted and aligned with the wall of LAA orifice; **c** 3rd oblique plane (double-oblique) where the enface view of the LAA is visualized, and measurements are taken for the widest and narrowest dimensions; and **d** measurement of the depth of the LAA for WATCHMAN implantation

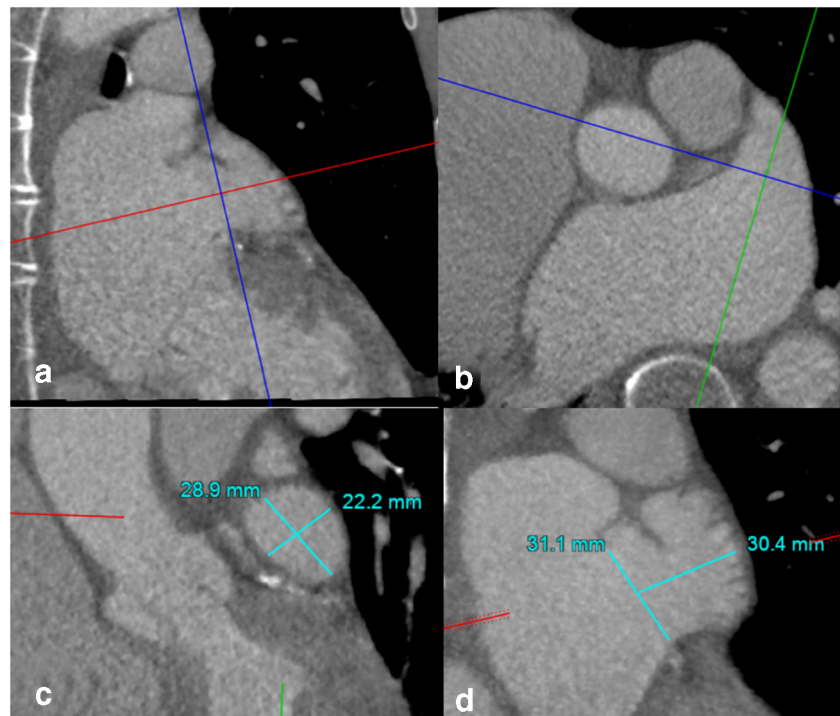
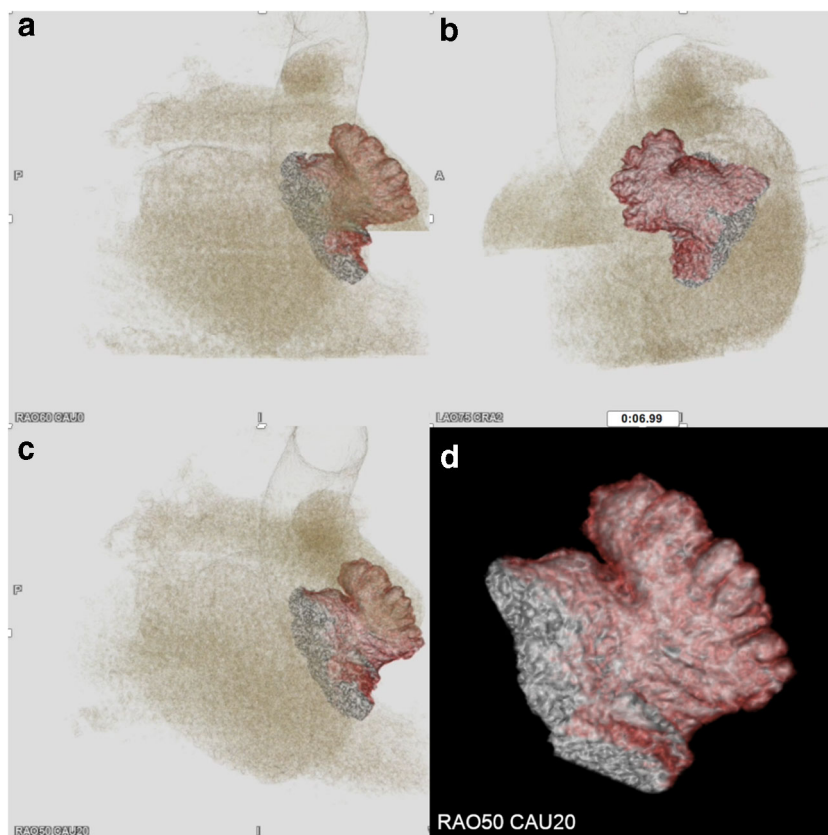


Fig. 2 3D volume rendered images of the same LAA in different projections with the Vitrea workstation: **a** RAO60, **b** LAO75 and cranial2, **c** RAO50 and caudal 20, and **d** dedicated 3D image of the LAA at RAO50 and caudal20 projection



± 4.7 mm and 24.6 ± 5.0 mm, $p = 0.9$) or LAA depth (19.5 ± 2.3 mm and 19.7 ± 2.3 mm, $p = 0.9$), though LAA volume could not be measured directly by 3D-TEE as opposed to CTA. Nucifora et al. [14] evaluated 46 patients who underwent CTA, 3D-TEE, and 2D-TEE and demonstrated excellent correlation between CTA and 3D-TEE ($r = 0.92$, 95% CI 0.85–0.95) compared with CTA and 2D-TEE ($r = 0.72$, 95% CI 0.54–0.83), though overall 2D-TEE and 3D-TEE underestimated LAA orifice area compared with CTA based on Bland Altman analysis.

Budge et al. found that planar CT reconstructions yielded smaller mean orifice diameter compared with 3D segmented CT reconstruction [15]. Wang and colleagues [8] found that pre-procedural imaging utilizing high-resolution gated CTA was associated with fewer device implantations per procedure and a 100% successful device implantation rate, at 1.2 devices/procedure in the study compared with 1.8 devices/procedure in the PROTECT-AF study [5]. In their initial retrospective study, subsequently followed by prospective study (PRO3DLAAO), Wang et al. found that CT sizing of the LAA was consistently larger than 2D and 3D-TEE and that 2D- and 3D-TEE consistently undersized the LAA on the order of 2–3 mm in maximal width size as compared to CTA measurements [8]. Application of CT procedural planning was directly correlated to elimination of the “Early Operator Learning Curve” witnessed in the first half of the PROTECT-AF studies

and resulted in 100% successful implant rate of the WATCHMAN device without complications [8]. Most importantly, these two studies demonstrated the application of pre-procedural CT resulted in a reduction in number of catheters used intraprocedurally, decrease in overall fluoroscopy time, and more efficient procedure time and turnover time.

3D Printing

Due to the ability to produce hands-on live prints, 3D printing has become increasingly applied to procedural planning in structural heart interventions. After a high-resolution ECG-gated CTA is obtained, the data can be processed on a multimodality workstation into segments and imported into a 3D software platform to be converted into 3D printable standard tessellation language to print a 3D relief. A cast is then made creating the final 3D print, which can be used in ex vivo studies for simulation of LAA device implantation, as first reported by Otton et al. in 2015 [16]. Hell et al. [17] performed CT analysis and printing on 22 patients and simulated LAA device implantation with the WATCHMAN device. The 3D predicted and actual implanted size was in agreement in 21/22 (95%) cases with one case being undersized requiring recapture and successful placement of a larger device. In contrast, CT-based device size prediction was in agreement with implanted device size in 17/22 cases (77%)

while TEE sizes were generally undersized, with implanted device agreement in only 12 cases (55%). Obasare et al. [18] reported similar results. A study of 29 patients [19] found that 3D printing provided reliable device sizing for the Amplatzer Amulet device but was less accurate at predicting sizing for the WATCHMAN device, though the number of devices attempted per procedure was not reported.

Safety/Efficacy

The safety profile of LAA closure has improved dramatically since the early clinical trials. In the early experience with PROTECT-AF study, procedure-related adverse events included pericardial tamponade requiring intervention (4%) and stroke (1.1%) [5]. In the PREVAIL [3] trial, 1.9% of study patients had a pericardial effusion requiring intervention. Safely outcomes continued to improve in the early commercial experience in the USA [20], with a major periprocedural complication rate of < 1.5%, including 1.0% pericardial tamponade and device embolization 0.25%. These improvements may be partially attributed to increasing operator experience and industry sponsored training of new operators [21]. As the safety profile of LAA closure continues to improve, one continued concern is device-related thrombosis (DRT) which had been estimated to occur at a rate of ~4% [22] and is associated with higher rates of stroke and/or transient ischemic attack [23]. Interestingly, a deep implant was found to be associated with DRT in two small studies [24, 25]. While this may be considered hypothesis generating rather than definitive given the small number of cases, it is reasonable to assume that the larger LAA size measured on CTA may be helpful in avoiding deep implant and thus providing a modifiable risk factor for avoiding DRT.

Proper device sizing on CTA may also reduce the incidence of peri-device leak. In a single-center analysis of 6 patients with peri-device leak following LAA closure with Amplatzer Cardiac Plug (St. Jude Medical, Minneapolis, MN) and Coherex WaveCrest (Salt Lake City, UT), Conti et al. [26] analyzed the pre-procedural CTA and created 3D prints after device implant. Undersizing of the LAA was found to be present in 100% (6/6) of patients with LAA peri-device leak and 34% of control patients (5/14). One patient suffered device migration in addition to leak [26].

Conclusions

The safety profile of LAA closure has improved dramatically and efficacy of stroke prevention with this procedure had been established. The next frontier in LAA closure should be dedicated to optimizing procedural safety by minimizing device exchanges, shortening procedure duration and appropriate device sizing to minimize DRT and peri-device leak. All of these

may be accomplished by optimal pre-procedural planning, in which CTA has a crucial role to play.

CT Imaging for Mitral Interventions

As catheter-based therapies continue to evolve for high-risk patients with failing mitral bioprostheses, severe mitral annular calcification (MAC), and prior mitral ring annuloplasties, CT imaging provides crucial planning advantages, namely by assisting sizing of the mitral annulus, and predicting left ventricular outflow tract (LVOT) obstruction (Fig. 3) [27].

CT Mitral Protocol

Mitral CT protocols involve contrast enhanced cardiac CTA using at least 64 detector row CT with retrospective ECG-gating, and similar tube current and voltage settings as described in LAA CT imaging. Image postprocessing at 10% intervals from 5 to 95% of the cardiac phase is obtained at 1.25 mm slice thickness. The CT DICOM images are transferred to a post-processing imaging workstation such as VitreaWorkstation™ (Vital, Toshiba Medical Systems Group Company, the Netherlands), Aquarius Workstation (TeraRecon Inc., Foster City, CA), Brilliance Workspace (Philips Healthcare, Andover, MA), 3mensio software (3mensio Medical Imaging, the Netherlands), and Mimics Materialize (Mimics, Materialize, Leuven, Belgium) [28, 29].

Mitral Annular Sizing

The mitral annular plane is identified by finding the basal most insertion of the mitral leaflets during mid to late diastole. Using the double-oblique method, crosshairs are placed in the coronal and sagittal planes at the level of the mitral leaflet insertion and the mitral annulus area can then be calculated in the double-oblique axial plane. For existing degenerative mitral ring/bioprostheses, the prosthesis-artifact edge is used. Based on the calculated mitral annular area, the appropriate transcatheter heart valve may be identified.

Risk of LVOT Obstruction

In transcatheter mitral valve replacement (TMVR), implantation of the mitral prosthesis causes permanent displacement of the anterior mitral leaflet towards the LVOT, which may result in critical LVOT obstruction [29]. LVOT obstruction has been described to occur in 9–22% of patients undergoing TMVR in native rings and accounts for > 50% exclusion from clinical trial participation in the setting of TMVR for valve in MAC [28–32]. The pre-procedural CT is used to calculate baseline and predicted “neo-LVOT areas” in order to predict the risk of LVOT obstruction [29]. In native annular calcification and

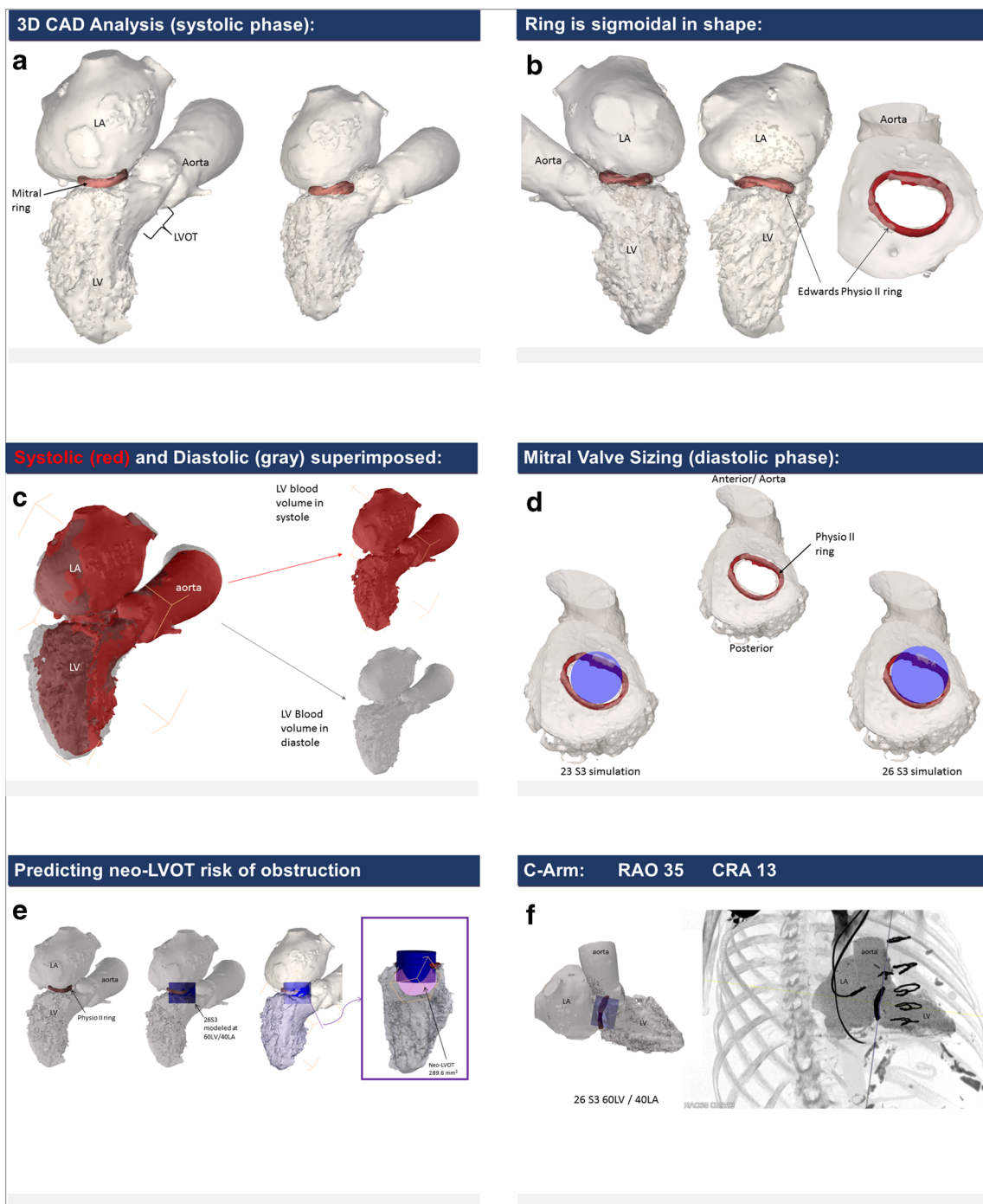


Fig. 3 CT imaging provides crucial planning advantages, namely by assisting sizing of the mitral annulus, and predicting LVOT obstruction

mitral rings, the transcatheter heart valve (THV) landing zone is defined in the axial plane as the point of maximal constriction between the anterior and posterior portions of the mitral annulus or ring. The THV is then modeled to deploy at 80% ventricular to the landing zone and again at 60% ventricular to the landing zone and neo-LVOT measurements are obtained at both deployment depths. In surgical bioprosthetic valves, a 0% deployment is defined as lining the virtual THV to the ventricular edge of the surgical valve. Neo-LVOT calculations

are determined at 0% deployment and again with the THV 20% ventricular to the ventricular edge of the surgical bioprosthesis [29].

A retrospective analysis of 38 patients [28] undergoing TMVR has determined predicted “neo-LVOT” area of < 189.4 mm² to have a 100% sensitivity and 96.8% specificity for LVOT obstruction (defined as gradient post-TMVR increase by 10 mmHg from baseline) (AUC 0.986, 95% CI 0.88–1.0, $p < 0.0001$). Post-TMVR CT found that the actual

neo-LVOT correlated well with predicted neo-LVOT area (Pearson correlation coefficient (R^2) 0.82, $p < 0.0001$). In some instances, a more acute aorto-mitral angle may also predispose to LVOT obstruction by causing the THV to protrude more significantly into the LVOT; however, this is not a universal scenario [29]. Other described risk factors include longer anterior mitral leaflet (AML) length (i.e., > 30 mm) [33], which may result in systolic anterior motion of the native leaflet tips and/or obstruction of flow into the THV itself, causing functional mitral stenosis. These patients may be referred for adjunctive preparatory therapies, such as pre-emptive alcohol septal ablation or the LAMPOON procedure. Alcohol septal ablation in patients with appropriate left ventricular septal anatomy and coronary anatomy is helpful in improving LVOT size and blood flow, but often involves a waiting period of 4–6 weeks prior to THV implant to allow for ventricular remodeling [32].

The LAMPOON technique [34] involves puncture of the AML by a coronary guidewire, followed by laceration and splitting of the AML under electrocautery parallel to the vertical length of the AML. The area between the two newly created AML partial leaflets allows blood flow out the LVOT, effectively enlarging the “new-LVOT” post-THV deployment. An early feasibility study in 5 patients demonstrated that the LAMPOON technique may be safely accomplished in a range of patient anatomies [34]. However, despite LAMPOON, not all patients may qualify for TMVR, as the existing skirt of the implanted THV inherently cannot be lacerated during this procedure and will result in LVOT obstruction if the “skirt neo-LVOT” is < 150 mm² [35].

Conclusions

As in the TAVR sphere, CT for preparation of transcatheter mitral procedures is crucial in identifying appropriate candidates for TMVR, including determination of THV size and appropriate patient anatomy. Patients identified by CT to have challenging anatomy may benefit from adjunctive therapies such as LAMPOON and alcohol septal ablation.

Compliance with Ethical Standards

Conflict of Interest All authors declare no conflict of interest.

Human and Animal Rights and Informed Consent This article does not contain any studies with human or animal subjects performed by any of the authors.

References

- Colilla S, Crow A, Petkun W, Singer DE, Simon T, Liu X. Estimates of current and future incidence and prevalence of atrial fibrillation in the U.S. adult population. *Am J Cardiol*. 2013 [cited 2018 Dec 30];112(8):1142–7. Available from: <https://www.sciencedirect.com/science/article/pii/S0002914913012885>.
- Blackshear JL, Odell JA. Appendage obliteration to reduce stroke in cardiac surgical patients with atrial fibrillation. *Ann Thorac Surg*. 1996 [cited 2018 Dec 30];61(2):755–9. Available from: <https://www.sciencedirect.com/science/article/pii/000349759500887X>.
- Doshi SK, Huber K, Reddy VY. Prospective randomized evaluation of the Watchman left atrial appendage closure device in patients with atrial fibrillation versus long-term warfarin therapy. *J Am Coll Cardiol*. 2014;64(1):1–12. <https://doi.org/10.1016/j.jacc.2014.04.029>.
- Wang YAN, Biase LDI, Horton RP. Left atrial appendage studied by computed tomography to help planning for appendage closure device placement.
- Singh SM, Douglas PS, Reddy VY. The incidence and long-term clinical outcome of iatrogenic atrial septal defects secondary to transseptal catheterization with a 12F transseptal sheath. *Circ Arrhythmia Electrophysiol*. 2011;4(2):166–71.
- Patel AR, Fatemi ONP, et al. Cardiac cycle-dependent left atrial dynamics: implications for catheter ablation of atrial fibrillation. *Heart Rhythm*. 2008;5:787–93.
- Saw J, Lopes P, Reisman M, McLaughlin P, Nicolau S, Bezerra HG. Cardiac computed tomography angiography for left atrial appendage closure. *Can J Cardiol*. 2016;32(8):1033. <https://doi.org/10.1016/j.cjca.2015.09.020>.
- Wang DD, Eng M, Kupsy D, Bfa EM, Bfa MF, Rahman M, et al. Application of 3-dimensional computed tomographic image guidance to WATCHMAN implantation and impact on early operator learning curve. *JACC Cardiovasc Interv*. 2016;9(22):2329–40. <https://doi.org/10.1016/j.jcin.2016.07.038>.
- Zhou Q, Song H, Zhang L, Deng Q, Chen J, Hu B, et al. Roles of real-time three-dimensional transesophageal echocardiography in peri-operation of transcatheter left atrial appendage closure. 2017;4(September 2016).
- Saw J, Fahmy P, Ch MBB, Spencer R, Prakash R, McLaughlin P, et al. Comparing measurements of CT angiography, TEE, and fluoroscopy of the left atrial appendage for percutaneous closure. *J Cardiovasc Electrophysiol*. 2016;27:414–22.
- Chow DHF, Bieliauskas G, Sawaya FJ, Millan-iturbe O, Kofoed KF, Søndergaard L, et al. A comparative study of different imaging modalities for successful percutaneous left atrial appendage closure. 2017.
- Rajwani A, Nelson AJ, Shirazi MG, Disney PJS, Teo KSL, Wong DTL, et al. CT sizing for left atrial appendage closure is associated with favourable outcomes for procedural safety. 2017;1361–8.
- Yosefy C, Laish-farkash A, Ph D, Azhibekov Y, Khalameizer V, Brodtkin B, et al. A new method for direct three-dimensional measurement of left atrial appendage dimensions during transesophageal echocardiography. 2015;13–5.
- Nucifora G, Faletra FF, Pasotti E. Evaluation of the left atrial appendage with real-time 3-dimensional transesophageal echocardiography implications for catheter-based left atrial appendage closure. 2011;514–23.
- Budge LP, Shaffer KM, Moorman JR, Lake DE, Ferguson JD, Mangrum JM. Analysis of in vivo left atrial appendage morphology in patients with atrial fibrillation: a direct comparison of transesophageal echocardiography, planar cardiac CT, and segmented three-dimensional cardiac CT. *J Interv Card Electrophysiol*. 2008;23(2): 87–93.
- Ottom JM, Spina R, Sulas R, Subbiah R, Jacobs N, Muller DW, et al. Left atrial appendage closure guided by personalized 3D-printed cardiac reconstruction. *J Am Coll Cardiol Cardiovasc Interv*. 2015;8(7):1004–6.
- Hell MM, Achenbach S, Yoo IS, Franke J, Blachutzik F, Roether J, et al. 3D printing for sizing left atrial appendage closure device : head-to-head comparison with computed tomography and

- transoesophageal echocardiography. *EuroIntervention*. 2017;13:1234–41.
18. Obasare E, Mainigi SK, Morris DL, Slipczuk L, Goykhman I, Friend E, et al. CT based 3D printing is superior to transesophageal echocardiography for pre-procedure planning in left atrial appendage device closure. *Int J Cardiovasc Imaging*. 2018;34(5):821–31. <https://doi.org/10.1007/s10554-017-1289-6>.
 19. Goitein O, Fink N, Guetta V, Beinart R. Printed MDCT 3D models for prediction of left atrial appendage (LAA) occluder device size: a feasibility study. 1076–9.
 20. Reddy VY, Gibson DN, Kar S, Neill WO, Doshi SK, Horton RP, et al. Post-approval U.S. experience with left atrial appendage closure for stroke prevention in atrial fibrillation. *J Am Coll Cardiol*. 2017;69(3):253–61. <https://doi.org/10.1016/j.jacc.2016.10.010>.
 21. Saw J, Price MJ. Assessing the safety of early. *J Am Coll Cardiol*. 2017;69(3):262–4. <https://doi.org/10.1016/j.jacc.2016.10.019>.
 22. Alkhouli M, Busu T, Shah K, Osman M, Alqahtani F, Raybuck B. Incidence and clinical impact of device-related thrombus following percutaneous left atrial appendage occlusion. *JACC Clin Electrophysiol*. 2018;4(12).
 23. Fauchier L, Cinaud A, Lepillier A, Pierre B, Abbey S, Fatemi M, et al. Device-related thrombosis after percutaneous left atrial appendage occlusion for atrial fibrillation. 2018;71(14).
 24. Pracon R, Bangalore S, Dzielinska Z. Structural heart disease device thrombosis after percutaneous left atrial appendage occlusion is related to patient and procedural characteristics but not to duration of postimplantation dual antiplatelet therapy. 2018;1–7.
 25. Kaneko H, Neuss M, Weissenborn J, Butter C. Predictors of thrombus formation after percutaneous left atrial appendage closure using the WATCHMAN device. *Heart Vessel*. 2017;32(9):1137–43.
 26. Conti M, Marconi S, Muscogiuri G, Guglielmo M, Baggiano A, Italiano G, et al. Left atrial appendage closure guided by 3D computed tomography printing technology: a case control study. *J Cardiovasc Comput Tomogr*. 2018;1–4. Available from: <https://doi.org/10.1016/j.jcct.2018.10.024>.
 27. Eng MH, Wang DD. Transseptal transcatheter mitral valve replacement for post-surgical mitral failures. *Interv Cardiol Rev*. 2018;13(2):77–80.
 28. Wang DD, Eng MH, Greenbaum AB, Myers E, Forbes M, Karabon P, et al. Validating a prediction modeling tool for left ventricular outflow tract (LVOT) obstruction after transcatheter mitral valve replacement (TMVR). *Catheter Cardiovasc Interv*. 2018;92(2):379–87.
 29. Wang DD, Eng M, Greenbaum A, Myers E, Forbes M, Pantelic M, et al. Obstruction after TMVR. *JACC Cardiovasc Imaging*. 2017;9(11):1349–52.
 30. Guerrero M, Urena M, Himbert D, Wang DD, Eleid M, Kodali S, et al. 1-year outcomes of transcatheter mitral valve replacement in patients with severe mitral annular calcification. *J Am Coll Cardiol*. 2018;71(17):1841–53.
 31. Guerrero M, Dvir D, Himbert D, Urena M, Eleid M, Wang DD, et al. Transcatheter mitral valve replacement in native mitral valve disease with severe mitral annular calcification: results from the first multicenter global registry. *JACC Cardiovasc Interv*. 2016;9(13):1361–71.
 32. Guerrero M, Wang DD, Himbert D, Urena M, Pursnani A, Kaddissi G, et al. Short-term results of alcohol septal ablation as a bail-out strategy to treat severe left ventricular outflow tract obstruction after transcatheter mitral valve replacement in patients with severe mitral annular calcification. *Catheter Cardiovasc Interv*. 2017;90(7):1220–6.
 33. Greenbaum AB, Condado JF, Eng M, Lerakis S, Wang DD, Kim DW, et al. Long or redundant leaflet complicating transcatheter mitral valve replacement: case vignettes that advocate for removal or reduction of the anterior mitral leaflet. *Catheter Cardiovasc Interv*. 2018;92(3):627–32.
 34. Babaliaros VC, Greenbaum AB, Khan JM, Rogers T, Wang DD, Eng MH, et al. Intentional percutaneous laceration of the anterior mitral leaflet to prevent outflow obstruction during transcatheter mitral valve replacement: first-in-human experience. *JACC Cardiovasc Interv*. 2017;10(8):798–809.
 35. Khan JM, Rogers T, Babaliaros VC, Fusari M, Greenbaum AB, Lederman RJ. Predicting left ventricular outflow tract obstruction despite anterior mitral leaflet resection. *JACC Cardiovasc Imaging*. 2018;2613. Available from: <http://imaging.onlinejacc.org/content/early/2018/05/10/j.jcmg.2018.04.005.abstract>.

Publisher's Note Springer Nature remains neutral with regard to jurisdictional claims in published maps and institutional affiliations.